Relation between near–field and far–field properties of plasmonic Fano resonances

Benjamin Gallinet[1,2] **and Olivier J. F. Martin**[1,3]

[1]*Nanophotonics and Metrology Laboratory,*
Swiss Federal Institute of Technology Lausanne (EPFL), Switzerland
[2]*benjamin.gallinet@epfl.ch*
[3]*olivier.martin@epfl.ch*

http://www.nanophotonics.ch

Abstract: The relation between the near–field and far–field properties of plasmonic nanostructures that exhibit Fano resonances is investigated in detail. We show that specific features visible in the asymmetric lineshape far–field response of such structures originate from particular polarization distributions in their near–field. In particular we extract the central frequency and width of plasmonic Fano resonances and show that they cannot be directly found from far–field spectra. We also address the effect of the modes coupling onto the frequency, width, asymmetry and modulation depth of the Fano resonance. The methodology described in this article should be useful to analyze and design a broad variety of Fano plasmonic systems with tailored near–field and far–field spectral properties.

OCIS codes: (310.6628) Subwavelength structures, nanostructures; (240.6680) Surface plasmons; (260.5740) Resonance.

References and links

1. U. Fano, "Effects of configuration interaction on intensities and phase shifts,"Citations Classics **27**, 219 (1977).
2. U. Fano, "Effects of configuration interaction on intensities and phase shifts," Phys. Rev. **124**, 1866 (1961).
3. B. Luk'yanchuk, N. I. Zheludev, S. A. Maier, N. J. Halas, P. Nordlander, H. Giessen, and C. T. Chong, "The Fano resonance in plasmonic nanostructures and metamaterials," Nat. Mater. **9**, 707–715 (2010).
4. A. E. Miroshnichenko, S. Flach, and Y. S. Kivshar, "Fano resonances in nanoscale structures," Rev. Mod. Phys. **82**, 2257–2298 (2010).
5. E. Prodan, C. Radloff, N. Halas, and P. Nordlander, "A hybridization model for the plasmon response of complex nanostructures," Science **302**, 419–422 (2003).
6. A. Christ, Y. Ekinci, H. H. Solak, N. A. Gippius, S. G. Tikhodeev, and O. J. F. Martin, "Controlling the Fano interference in a plasmonic lattice," Phys. Rev. B **76**, 201405 (2007).
7. N. A. Mirin, K. Bao, and P. Nordlander, "Fano Resonances in Plasmonic Nanoparticle Aggregates," J. Phys. Chem. A **113**, 4028–4034 (2009).
8. N. Liu, L. Langguth, T. Weiss, J. Kaestel, M. Fleischhauer, T. Pfau, and H. Giessen, "Plasmonic analogue of electromagnetically induced transparency at the drude damping limit," Nat. Mater. **8**, 758–762 (2009).
9. J. A. Fan, C. Wu, K. Bao, J. Bao, R. Bardhan, N. J. Halas, V. N. Manoharan, P. Nordlander, G. Shvets, and F. Capasso, "Self-assembled plasmonic nanoparticle clusters," Science **328**, 1135–1138 (2010).
10. K. Bao, N. A. Mirin, and P. Nordlander, "Fano resonances in planar silver nanosphere clusters," Appl. Phys. A, Mater. Sci. Process. **100**, 333–339 (2010).
11. Y. Sonnefraud, N. Verellen, H. Sobhani, G. A. E. Vandenbosch, V. V. Moshchalkov, P. Van Dorpe, P. Nordlander, and S. A. Maier, "Experimental realization of subradiant, superradiant, and fano resonances in ring/disk plasmonic nanocavities," ACS Nano **4**, 1664–1670 (2010).
12. Z.-J. Yang, Z.-S. Zhang, L.-H. Zhang, Q.-Q. Li, Z.-H. Hao, and Q.-Q. Wang, "Fano resonances in dipole-quadrupole plasmon coupling nanorod dimers," Opt. Lett. **36**, 1542–1544 (2011).

#151848 - $15.00 USD Received 27 Jul 2011; revised 16 Sep 2011; accepted 14 Oct 2011; published 24 Oct 2011

13. B. Gallinet and O. J. F. Martin, “Ab initio theory of Fano resonances in plasmonic nanostructures and metamaterials,” Phys. Rev. B **83**, 235427 (2011).
14. A. Christ, O. J. F. Martin, Y. Ekinci, N. A. Gippius, and S. G. Tikhodeev, “Symmetry breaking in a plasmonic metamaterial at optical wavelength,” Nano Lett. **8**, 2171–2175 (2008).
15. N. Verellen, P. Van Dorpe, D. Vercruysse, G. A. E. Vandenbosch, and V. V. Moshchalkov, “Dark and bright localized surface plasmons in nanocrosses,” Opt. Express **19**, 11034–11051 (2011).
16. S. Zhang, D. A. Genov, Y. Wang, M. Liu, and X. Zhang, “Plasmon-induced transparency in metamaterials,” Phys. Rev. Lett. **101**, 047401 (2008).
17. N. Verellen, Y. Sonnefraud, H. Sobhani, F. Hao, V. V. Moshchalkov, P. Van Dorpe, P. Nordlander, and S. A. Maier, “Fano resonances in individual coherent plasmonic nanocavities,” Nano Lett. **9**, 1663–1667 (2009).
18. B. Gallinet and O. J. F. Martin, “Scattering on plasmonic nanostructures arrays modeled with a surface integral formulation,” Photon. Nanostruct. **8**, 278–284 (2010).
19. B. Gallinet, A. M. Kern, and O. J. F. Martin, “Accurate and versatile modeling of electromagnetic scattering on periodic nanostructures with a surface integral approach,” J. Opt. Soc. Am. A **27**, 2261–2271 (2010).
20. A. M. Kern and O. J. F. Martin, “Surface integral formulation for 3D simulations of plasmonic and high permittivity nanostructures,” J. Opt. Soc. Am. A **26**, 732–740 (2009).
21. A. M. Kern and O. J. F. Martin, “Excitation and reemission of molecules near realistic plasmonic nanostructures,” Nano Lett. **11**, 482–487 (2011).
22. D. J. Bergman and M. I. Stockman, “Surface Plasmon Amplification by Stimulated Emission of Radiation: Quantum Generation of Coherent Surface Plasmons in Nanosystems,” Phys. Rev. Lett. **90**, 027402 (2003).
23. N. I. Zheludev, S. L. Prosvirnin, N. Papasimakis, and V. A. Fedotov, “Lasing spaser,” Nat. Photonics **2**, 351–354 (2008).
24. P. B. Johnson and R. W. Christy, “Optical-constants of noble-metals,” Phys. Rev. B **6**, 4370 (1972).

1. Introduction

In 1977, Ugo Fano recounted the circumstances which prompted him to develop an original formalism to describe asymmetric spectral lineshapes: ”Late in 1960, R.L. Platzman called to my attention a strikingly asymmetric line profile in an unpublished spectrum of energy transfers in electron collisions by Lassettre and coworkers. This spectrum appeared analogous to those I had interpreted in 1935. My reply to Platzman provided the opportunity for a modernized formulation of the analytical treatment” [1]. This seminal work, published in 1961 [2], has generated a very strong interest, first in the atomic and molecular spectroscopy scientific communities, where asymmetric spectral lines can be observed in experiments where the discrete excited state of an atom or molecule interacts with a continuum.

More recently, advances in nanofabrication techniques have given rise to a new family of structures where Fano resonances can be observed experimentally at optical frequencies. These structures rely on plasmonic materials and we refer the reader to Refs. [3, 4] which provide detailed reviews of the current state–of–the–art. This new family of Fano resonant structures can provide new insights into the mechanisms leading to asymmetric lineshapes. Indeed, the ”atoms” constituting such structures have typical extensions in the tens of nanometers. Therefore, it is possible to associate with each Fano resonance a specific near–field distribution and a polarization distribution in these ”atoms” [5–12].

In this paper, we specifically investigate the link between the near–field distribution and the spectral response of a plasmonic system exhibiting Fano resonances. In particular, we show that specific features visible in the far–field response of the structure originate from specific field and polarization distributions in the near–field.

2. Results and discussion

Fano resonances are built from the interference between a continuum of radiative waves and a non–radiative (i.e. dark) mode that are spectrally and spatially overlapping [3]. The radiative waves can for example be constructed from a radiative (bright) mode of a first plasmonic nanostructure, whose reflectance exhibits the following symmetric lorentzian lineshape as a function

#151848 - $15.00 USD Received 27 Jul 2011; revised 16 Sep 2011; accepted 14 Oct 2011; published 24 Oct 2011

of the frequency ω:

$$R_b(\omega) = \frac{a^2}{\left(\frac{\omega^2-\omega_s^2}{(W_s+\omega_s)^2-\omega_s^2}\right)^2+1}, \tag{1}$$

where a is the maximum amplitude of the resonance, ω_s the resonance frequency and W_s its spectral width for $W_s \ll \omega_s$. Contrary to a quantum mechanical formulation, the electromagnetic modes' eigenvalues are expressed in eV^2 and their resonance shape are expressed as function of ω^2 (see for instance Eq. (1) in Ref. [13]). However, for convenience we discuss from now on the central frequency and width of the resonance in eV. The first nanostructure supporting the lorentzian resonance must then be placed in close interaction with a second one supporting the dark mode. Alternatively, a single nanosystem can also produce a Fano resonance, provided that it supports two modes that can hybridize into a bright and a dark mode [3, 6, 14, 15]. The interference of these bright and dark modes leads to a Fano–like asymmetric resonance whose lineshape is given by [13]:

$$\sigma(\omega) = \frac{\left(\frac{\omega^2-\omega_a^2}{(W_a+\omega_a)^2-\omega_a^2}+q\right)^2+b}{\left(\frac{\omega^2-\omega_a^2}{(W_a+\omega_a)^2-\omega_a^2}\right)^2+1}. \tag{2}$$

where ω_a is the central spectral position, W_a the spectral width for $W_a \ll \omega_a$, q the asymmetry parameter introduced by Fano in his quantum theory [2], and b the modulation damping parameter appearing with intrinsic losses. Note that Eq. (2) is a generalization of the original Fano formula for systems with losses, such as plasmonic materials [13]. For the particular case $q = 0$, the lineshape of Eq. (2) becomes the one of an antiresonance centered around ω_a with minimum value b and width W_a. As the absolute value of the asymmetry parameter q increases, the lineshape of Eq. (2) becomes comparable to a lorentzian profile ($q = \pm\infty$). Equation (2) with constant parameters is valid in a small frequency interval around the frequency of a single resonant dark mode, and assumes that the dark mode's spectral width is smaller than the bright mode's spectral width [13]. The reflectance of the entire system is given by the product of the symmetric reflectance spectrum of the bright mode R_b [Eq. (1)] modulated by σ [Eq. (2)]:

$$R(\omega) = R_b(\omega)\sigma(\omega). \tag{3}$$

Let us now discuss the validity of Eq. (3). If two dark modes interact with the same continuum but their respective asymmetric lineshapes do not spectrally overlap, Eq. (3) becomes the product of the background resonance R_b with two independant lineshapes σ and σ'. For the case of two bright modes, where one does not interact with the dark mode, the additional bright mode alters the total reflectance R. The approach shown here is therefore valid only for a single bright and a single dark mode that are spectrally and spatially overlapping, and requires a preliminary insight into the eigenmode spectrum of the structure, as shown in Figure 2 of Ref. [13].

We now discuss how the near–field interactions within different plasmonic nanostructures building the Fano system relate to the far–field response given by Eq. (3). To this end, we consider the reflectance of a dolmen–type plasmonic nanostructure consisting of three metallic beams arranged as shown in Fig. 1(a) [16, 17]. The two parallel beams support a quadrupolar dark mode, while the third perpendicular beam supports a dipolar bright mode. The bright mode has a large spectral width due to radiative damping, and can be therefore considered as a continuum of radiative waves. The interference between the two modes leads to a Fano–type resonance. At frequency ω_s, the bright mode of the single beam is resonantly excited. The dark mode is perturbed by the coupling to the bright mode and resonates at a frequency ω_a slightly detuned from its original resonance frequency, and the width of this resonance is determined

#151848 - $15.00 USD Received 27 Jul 2011; revised 16 Sep 2011; accepted 14 Oct 2011; published 24 Oct 2011

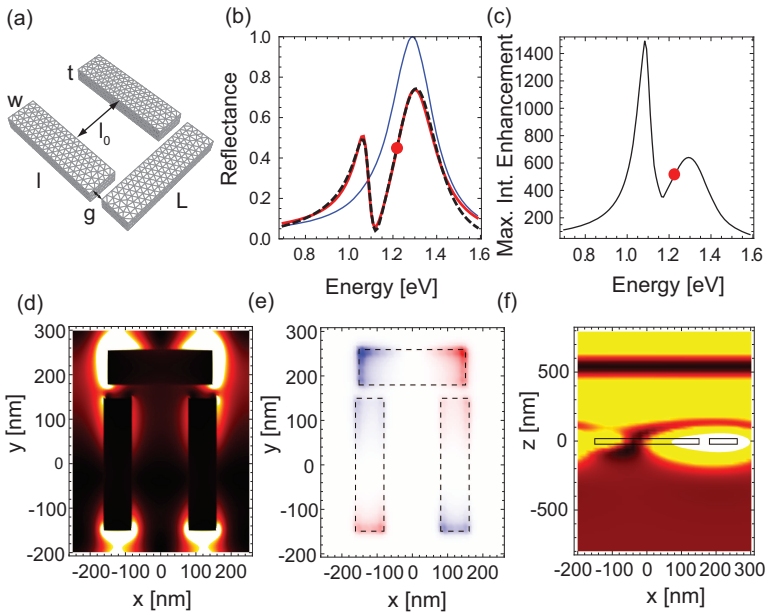

Fig. 1. (Media 1) Fano resonance in a array of dolmen–type gold nanostructures. (a) Sketch of the structure, dimensions: $w = 40$ nm, $l_0 = 160$ nm, $t = 80$ nm, $g = 30$ nm and $l = L = 300$ nm. (b) Reflectance at normal incidence for an x–polarized electric field propagating in the $-z$–direction, as a function of the illumination energy. Black dashed line: numerical simulations; thick red solid line: fit with Eq. (3); thin blue solid line: bright mode resonance extracted from the fit [Eq. (1)]. (c) Maximum intensity enhancement as a function of the illumination energy. (d) Normalized intensity enhancement in a plane through the center of the structure ($z = 0$, colorscale: black $\rightarrow$ 0 and white $\rightarrow$ 1). (e) Normalized amplitude of the z–component of the instantaneous electric field 5 nm above the structure (colorscale: blue $\rightarrow$ -1 and red $\rightarrow$ 1). (f) Normalized intensity enhancement in a $x = 200$ nm plane (colorscale: black $\rightarrow$ 0 and white $\rightarrow$ 1).

by both the modes coupling and intrinsic losses [13]. The movie in Fig. 1 shows the evolution of the system as a function of the illumination energy. The dolmens are arranged in vacuum in a two–dimensional array with period 500 nm. The material is chosen to satisfy a Drude model with plasma frequency $\omega_p = 1.37 \times 10^{16}$ s^{-1} and damping $\gamma = 1.23 \times 10^{14}$ s^{-1}, which corresponds to the dielectric permittivity of gold. The black dashed line in Fig. 1(b) shows the reflectance spectrum of the array under normal illumination, calculated using the surface integral method [18, 19]. This spectrum is then fitted with Eq. (3), where the constrain $a < 1$ is imposed in order to fulfill energy conservation. The fit parameters are $a = 1.00$, $\omega_s = 1.29$ eV, $W_s = 0.12$ eV, $\omega_a = 1.08$ eV, $W_a = 0.03$ eV, $q = -0.96$, $b = 0.34$, and the corresponding curve is drawn as a solid red line in Fig. 1(b). In Fig. 2(a), the same geometry and illumination conditions are considered, but for a single dolmen instead of an array. Due to retardation effect, the quadrupolar mode can be excited from the far–field at grazing incidence [17], and by reciprocity cannot be considered as completely dark. In the geometry of Fig. 1 and Fig. 2(b), positioning the structures in a subwavelength array suppresses radiation at a non normal angle and ensures that the quadrupolar mode is a true dark mode. As a result, the fit of Fig. 2(a) (with parameters $a = 2.63$, $\omega_s = 1.33$ eV, $W_s = 0.10$ eV, $\omega_a = 0.98$ eV, $W_a = 0.05$ eV, $q = -1.83$, $b = 1.80$) is not as satisfying as the fit of Fig. 2(b) (with parameters $a = 1.00$, $\omega_s = 1.29$ eV, $W_s = 0.03$ eV,

#151848 - $15.00 USD Received 27 Jul 2011; revised 16 Sep 2011; accepted 14 Oct 2011; published 24 Oct 2011

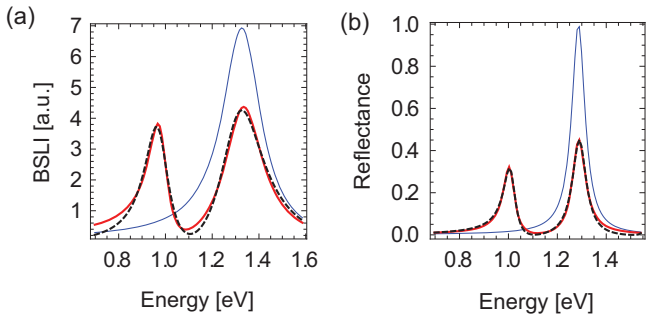

Fig. 2. (a) Back Scattered Light Intensity (BSLI) of a single dolmen nanostructure with the geometry and illumination conditions of Fig. 1. (b) Reflectance of an array of dolmen nanostructures with the geometry and illumination conditions of Fig. 1, placed in a two dimensional array of period 800 nm. Black dashed line: numerical simulations; thick red solid line: fit with Eq. (3); thin blue solid line: bright mode resonance extracted from the fit [Eq. (1)].

$\omega_a = 1.00$ eV, $W_a = 0.03$ eV, $q = -3.88$, $b = 3.75$) or the fit of Fig. 1(b). In a periodic array, near–field interactions between nearest neighbors have to be taken into account, as will be seen later.

For calculating the spectrum in Fig. 1(c), the electric field is sampled at each frequency on a 5 nm homogeneous grid of points at 1 nm from the nanostructures surface. The surface integral method used in this work calculates the field semi–analytically at positions arbitrarily close to surfaces and therefore does not suffer from numerical inaccuracies [19–21]. The maximal value of the electric intensity for each frequency is reported in Fig. 1(c). The maximal near–field enhancement is found at 1.08 eV, which corresponds exactly to the resonance frequency ω_a found from the fit in Fig. 1(b). The points of maximal near-field enhancement are located at $(x,z) = (\pm 80, 0)$nm, i.e. at the two top interior corners of the beam pair [Fig. 1(d)]. Figures 1(d) to (f), which show the normalized intensity enhancement and the corresponding polarization charges through the structure, indicate that the quadrupolar mode of the double beam structure is resonantly excited at ω_a. The second peak in Fig. 1(c) corresponds to the excitation of the bright mode. The maximum intensity enhancement is found at 1.29 eV, which also corresponds exactly to its resonance frequency ω_s found from the fit in Fig. 1(b). The maximum intensity enhancement observed at ω_a is about 2.3 times the maximum intensity enhancement observed for the excitation of the bright mode at ω_s. This significant near–field enhancement originates from the fact that the dark mode does not suffer from radiative losses and is therefore able to store a larger amount of electromagnetic energy than the bright mode. Figure 1(e) also shows that the phase of the instantaneous electric field switches by π around ω_a. Two pathways have to be considered in the excitation from the far–field: the direct excitation of the bright mode and the excitation of the dark mode through its coupling to the bright mode. These two pathways interfere to produce the asymmetric lineshape observed in Fig. 1(b) around ω_a (Eq. (22) of [13]). Its degree of asymmetry is described by the q parameter, while the modulation damping by intrinsic losses is described by the b parameter. The latter prevents the reflectance spectrum to reach zero values and can be understood as the ratio of the energy that is lost in heat to the metallic structure, to the energy that is transferred from the continuum to the dark mode (see Section IV of [13] for a closed form expression of these parameters for the classical model of two coupled oscillators). In the minimum of the resonance spectrum (around 1.1 eV), the Fano interference opens a narrow transparency window for the incoming light. At this fre-

#151848 - $15.00 USD Received 27 Jul 2011; revised 16 Sep 2011; accepted 14 Oct 2011; published 24 Oct 2011

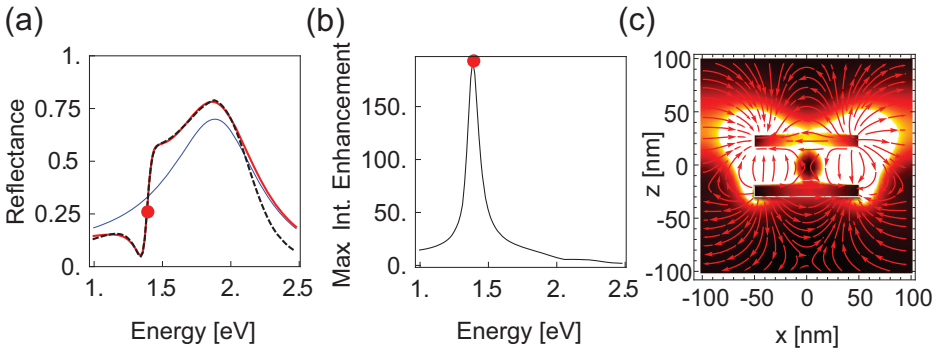

Fig. 3. (Media 2) Fano–like resonance in a metallic double grating. Each nanowire is infinite in y–direction and has a 100 nm length (x–direction) and a 15 nm thickness (z–direction). The wires are made of gold (data from Johnson and Christie [24]) and embedded in a silica matrix (refractive index 1.46). Their vertical spacing is 30 nm and are placed in a one–dimensional lattice with period 200 nm. The system is illuminated at normal incidence with a field propagating in the $-z$–direction, with the magnetic field polarized along the y–direction. (a) Reflectance as a function of the illumination energy. Black dashed line: numerical simulations; thick red solid line: fit with Eq. (3); thin blue solid line: bright mode resonance extracted from the fit [Eq. (1)]. (b) Maximum intensity enhancement as a function of the illumination energy. (c) Normalized intensity enhancement in the cross section plane (colorscale: black $\rightarrow$ 0 and white $\rightarrow$ 1).

quency, the maximum intensity enhancement is only about 1.9 times the maximum intensity enhancement observed for the excitation of the bright mode at ω_s. This shows that locating the central resonance frequency ω_a is a critical point for applications such as refractive index sensing or lasing [3, 22, 23].

This interplay between near–field and far–field is also observed in Fig. 3 for a metallic double grating structure. In this nanosystem the hybridization of the plasmon modes of each nanowire leads to the formation of a bonding antisymmetric mode and an antibonding symmetric mode which are respectively non-radiative and radiative [14]. These two modes are supported by the same nanostructure and therefore cannot be assigned to different parts of the nanosystem, as was the case for the dolmen structure in Fig. 1. However, it is still possible to perform the fit to Eq. (3) and extract the background resonance from the bright mode [blue thin solid curve in Fig. 3(a)]. The fit parameters are $a = 0.84$, $\omega_s = 1.88$ eV, $W_s = 0.37$ eV, $\omega_a = 1.38$ eV, $W_a = 0.13$ eV, $q = 0.66$, and $b = 0.27$. The electric field is sampled at each frequency on a 1 nm homogeneous grid of positions at 1 nm from the nanostructures surface. The maximal electric field intensity for each frequency is then reported in Fig. 3(b). The maximal intensity in the spectrum of Fig. 3(b) is fitted with a lorentzian profile similar to Eq. (1). Its central frequency is found at approximately 1.39 eV and has a width of 0.06 eV. These values agree well with the values of ω_a and W_a found from the fit of Fig. 3(a). At this frequency, the maximum intensity enhancement is about 16 times the one observed for the excitation of the bright mode at ω_s. This lets us conclude that the dark mode is resonantly excited at this frequency. The near-field distribution in Fig. 3(c) also indicates a quadrupolar charges configuration in the structure at ω_a. The points of maximal near-field enhancement are located at $(x,z) = (\pm 50, 14)$nm, i.e. at the two bottom corners of the top nanoparticle. Let us emphasize that it is not possible to determine *a priori* the resonance frequency ω_a from a Fano resonance spectrum such as the black dashed curve in Fig. 1(b) or in Fig. 3(a), since its shape is determined by many parameters and ω_a does

#151848 - $15.00 USD Received 27 Jul 2011; revised 16 Sep 2011; accepted 14 Oct 2011; published 24 Oct 2011

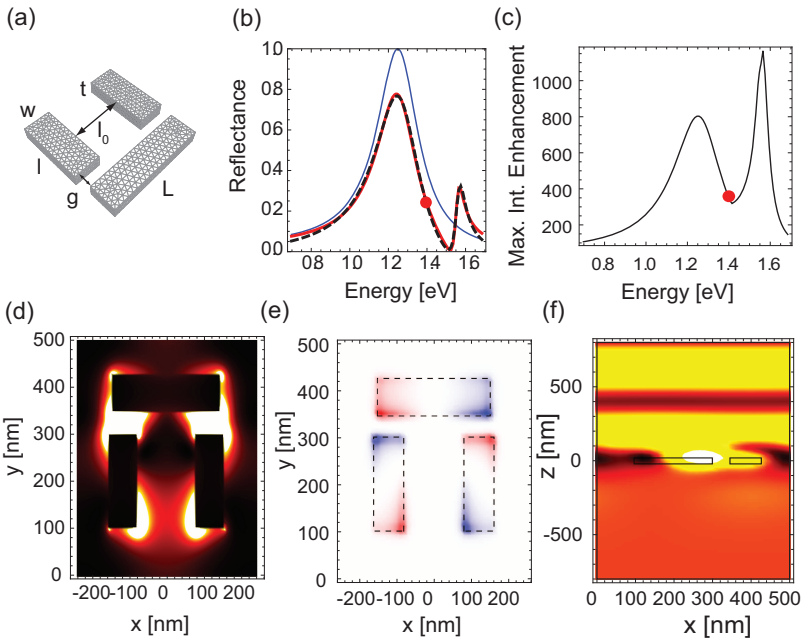

Fig. 4. (Media 3) Fano resonance in a dolmen gold nanostructure. (a) Sketch of the structure, dimensions: $w = 40$ nm, $l_0 = 160$ nm, $t = 80$ nm, $g = 45$ nm, $l = 200$ nm, and $L = 300$ nm. (b) Reflectance at normal incidence for an x–polarized electric field propagating in the $-z$–direction, as a function of the illumination energy. Black dashed line: numerical simulations; thick red solid line: fit with Eq. (3); thin blue solid line: bright mode resonance extracted from the fit [Eq. (1)]. (c) Maximum intensity enhancement as a function of the illumination energy. (d) Normalized intensity enhancement in a plane through the center of the structure ($z = 0$, colorscale: black $\rightarrow$ 0 and white $\rightarrow$ 1). (e) Normalized amplitude of the z–component of the instantaneous electric field 5 nm above the structure (colorscale: blue $\rightarrow$ -1 and red $\rightarrow$ 1). (f) Normalized intensity enhancement in a $x = 200$ nm plane (colorscale: black $\rightarrow$ 0 and white $\rightarrow$ 1).

not correspond to a specific point in the spectrum (for instance a local minimum or maximum). However, the fit with Eq. (3) is able to extract ω_a easily, without detailed knowledge of the near–field interactions.

We now turn our attention to the influence of the respective spectral positions of the bright and dark modes. In Fig. 4, the length of the two parallel beams is shortened in order to blue shift the dark mode's resonance to frequencies above ω_s. The same procedure as in Fig. 1 is repeated for this structure. The fit parameters are now $a = 1.00$, $\omega_s = 1.25$ eV, $W_s = 0.12$ eV, $\omega_a = 1.55$ eV, $W_a = 0.02$ eV, $q = 1.30$, and $b = 0.15$. The asymmetric resonance appears now on the other shoulder of the bright mode's resonance, compare Fig. 1(b) and Fig. 4(b). The shift in the modes frequency is a function of their spectral detuning. As a result, the resonance frequency of the bright mode red shifts from 1.38 eV to 1.25 eV. Since the asymmetry parameter depends on the frequency difference $\omega_a^2 - \omega_s^2$ [13], it reverses its sign from Fig. 1 to Fig. 4, which now makes the resonance appearing as a dip followed by a peak for higher frequencies. The fit with Eq. (3) also enables extracting the resonance frequency ω_a in this configuration. The resonance is now at a higher frequency than the dip's frequency, because the asymmetry parameter is positive. The absolute value of q is larger than in the case of Fig. 1, which pushes

#151848 - $15.00 USD Received 27 Jul 2011; revised 16 Sep 2011; accepted 14 Oct 2011; published 24 Oct 2011

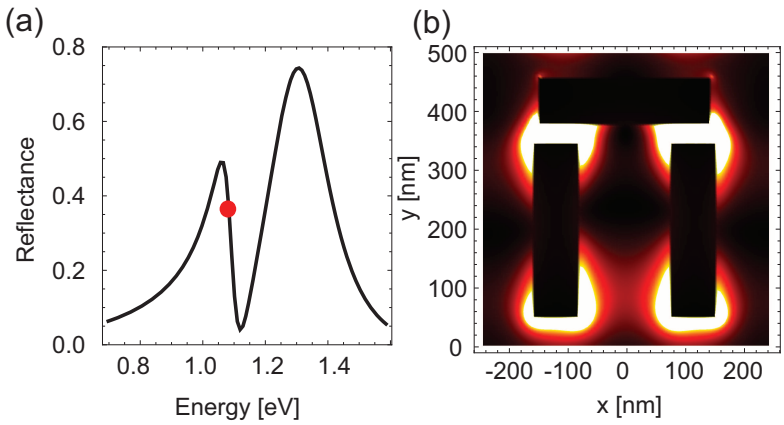

Fig. 5. (Media 4) Influence of modes coupling on the resonance line shape for dolmen gold nanostructures with dimensions $w = 40$ nm, $l_0 = 160$ nm, $t = 80$ nm, and $l = L = 300$ nm. The coupling is changed by tuning the gap size g from 15 nm to 60 nm in steps of 5 nm. (a) Reflectance at normal incidence for an x–polarized electric field propagating in the $-z$–direction, as a function of the illumination energy. The red dot indicates the Fano resonance frequency position. (b) Normalized intensity enhancement in a plane through the center of the structure at the Fano resonance frequency ($z = 0$, colorscale: black $\rightarrow$ 0 and white $\rightarrow$ 1).

the resonance frequency towards the second reflectance peak (Fig. 1 in Ref. [2]). The electric field is sampled at each frequency on a 5 nm homogeneous grid at 1 nm from the nanostructures surface. The maximal electric field intensity for each frequency is then reported in Fig. 4(c). The largest field enhancement, corresponding to the resonant excitation of the dark mode, appears at approximately 1.57 eV. The points of maximal near-field enhancement are located at $(x,z) = (\pm 161, 100)$nm, i.e. at the two exterior bottom corners of the beam pair. A phase shift of the dark mode similar to the case of Fig. 1 occurs in a frequency region around ω_a [Fig. 4(e)]. The first peak in Fig. 4(c) is attributed to the bright mode's excitation and is centered around 1.25 eV, in agreement with the value $\omega_s = 1.25$ eV found from the fit.

It has been observed [16, 17] and later theoretically demonstrated [13] that the coupling between the bright and dark modes plays an important role for controlling the line shape of Fano–like resonances. This dominant effect of coupling is described by the modulation damping parameter b giving the ratio between the power lost in the metallic structure and the power transferred from the bright mode to the dark mode. The near–field intensity enhancement maps in Figs. 1 and 4 indicate that the most efficient way to change the coupling is by tuning the gap size g between the single beam and the pair of parallel beams, Fig. 5. For high coupling, in the spectral minimum in the reflectance response, the Fano interference opens a narrow transparency window for the incoming light, whose magnitude depends on the b parameter. As g increases, the coupling between the two modes decreases, the b parameter drastically increases and the resonance modulation depth is reduced. As a result, the reflectance of the system approaches that of the bright mode alone [Fig. 5(a)]. This effect appears only in the presence of intrinsic losses and goes along with a reduction of the absolute value of the asymmetry parameter (from -1.68 for $g = 15$ nm to -0.21 for $g = 50$ nm). As the coupling decreases, the resonance becomes more symmetric and its frequency shifts towards the reflectance dip. In addition, the resonance frequency blue shifts, and converges to the non–perturbed resonance frequency of the dark mode [13]. The coupling of the dark mode to the bright mode opens a radiative decay

#151848 - $15.00 USD Received 27 Jul 2011; revised 16 Sep 2011; accepted 14 Oct 2011; published 24 Oct 2011

channel for the dark mode, which in turns widens the Fano resonance. Figure 5(b) shows the intensity enhancement in the structure at the resonance frequency ω_a extracted from a fit with Eq. (3); this frequency is indicated by a red dot in panel (a). The correlation between near–field and far–field is also verified in this case: as the two modes decouple, the power transfer between the two parallel beams and the third becomes less effective. This results in a decrease of the field intensity in the two parallel beams, leading finally to field enhancement solely at the extremities of the single beam, when both structures are decoupled and the Fano resonance has disappeared, $g \simeq 60$ nm (Fig. 5). As mentioned previously, the structures are placed in an array to ensure that the quadrupolar mode is a true dark mode. Although its subwavelength character does not produce grating effects, this configuration is accompanied by strong near–field interactions between nearest neighbors. The gap size of g =60 nm in Fig. 5 leading to a complete vanishing of the Fano resonance corresponds to a configuration for which the dipolar beam is placed at the same distance from its two adjacent beam pairs, i.e. to a configuration for which the array has a $y = 0$ symmetry plane. Moving the dipolar bar from this position induces the symmetry breaking required for the excitation of the dark mode, which explains the high sensitivity of the resonance lineshape to the gap size g.

3. Conclusion

We have investigated the relation between the near–field and far–field properties of plasmonic nanostructures that exhibit Fano resonances. By fitting reflectance spectra for different geometries with a general equation derived in Ref. [13] we have been able to determine the central frequency, width and modulation of the Fano resonance, and to further retrieve the shape of the bright mode in these systems. We have shown that the central frequency of the asymmetric modulation corresponds to the maximum near–field intensity enhancement in the structure, but does not correspond to a specific point of the reflectance spectrum (for instance a local minimum or maximum). We have also related the far–field spectrum to the near–field configuration of the bright and dark modes, and addressed the effect of their coupling to the frequency, width, asymmetry and modulation depth of the Fano resonance. The methodology described in this article should by useful to analyze and design a broad variety of Fano plasmonic systems with tailored near–field and far–field spectral properties.

Acknowledgments

Funding from the CSEM and the CCMX–Fanosense project as well as stimulating discussions with M. Schnieper and A. Stuck are gratefully acknowledged.

#151848 - $15.00 USD Received 27 Jul 2011; revised 16 Sep 2011; accepted 14 Oct 2011; published 24 Oct 2011